Current Biology, Vol. 15, 1276–1285, July 26, 2005, ©2005 Elsevier Ltd All rights reserved. DOI 10.1016/j.cub.2005.06.043

Cortactin Promotes Cell Motility by Enhancing Lamellipodial Persistence

Nicole S. Bryce,[1] Emily S. Clark,[2] Ja'Mes L. Leysath,[1] Joshua D. Currie,[1] Donna J. Webb,[3,4] and Alissa M. Weaver[1,2,*]
[1]Department of Cancer Biology
[2]Department of Pathology
Vanderbilt University Medical Center
Nashville, Tennessee 37232
[3]Department of Cell Biology
University of Virginia Health Sciences Center
Charlottesville, Virginia 22908

Summary

Background: Lamellipodial protrusion, which is the first step in cell movement, is driven by actin assembly and requires activity of the Arp2/3 actin-nucleating complex. However, it is unclear how actin assembly is dynamically regulated to support effective cell migration.
Results: Cells deficient in cortactin have impaired cell migration and invasion. Kymography analyses of live-cell imaging studies demonstrate that cortactin-knockdown cells have a selective defect in the persistence of lamellipodial protrusions. The motility and protrusion defects are fully rescued by cortactin molecules, provided both the Arp2/3 complex and F-actin binding sites are intact. Consistent with this requirement for simultaneous contacts with Arp2/3 and F-actin, cortactin is recruited by Arp2/3 complex to lamellipodia and binds with a higher affinity to ATP/ADP-Pi-F-actin than to ADP-F-actin. In situ labeling of lamellipodia revealed that the relative levels of free barbed ends of actin filaments are reduced by over 30% in the cortactin-knockdown cells; however, there is no change in Arp2/3-complex localization to lamellipodia. Cortactin-knockdown cells also have a selective defect in the assembly of new adhesions in protrusions, as assessed by analysis of GFP-paxillin dynamics in living cells.
Conclusions: Cortactin enhances lamellipodial persistence, at least in part through regulation of Arp2/3 complex. The presence of cortactin also enhances the rate of new adhesion formation in lamellipodia. In vivo, these functions may be important during directed cell motility.

Introduction

Lamellipodial protrusions determine the direction of cell movement and result from polymerization of branched-actin filaments against the plasma membrane [1]. To form this branched-actin network, which produces protrusive force, activated Arp2/3 complex binds to the side of an actin filament and nucleates daughter filaments [1–3]. Activation of Arp2/3 complex occurs in response to various signals, including growth factors, src family kinases, and rho GTPases, and is mediated by direct binding of nucleation-promoting factors (NPFs) [1]. Members of the Wiskott Aldrich Syndrome protein (WASp) family are the best-characterized NPFs [4]. A less-well-understood activator of Arp2/3 complex is cortactin, known to bind and activate Arp2/3 complex in purified-protein systems [5–7]. Cortactin activates Arp2/3 complex likely via a distinct mechanism involving interactions with actin filaments [6, 7], whereas WASps interact with G-actin [4]. Efficiency of cortactin activation is low but approaches that of WASps if its binding partner, WASp-interacting protein (WIP), is present [8]. Cortactin also enhances N-WASp activation of Arp2/3 complex in pyrene-actin-polymerization assays [6, 7] and inhibits debranching of in vitro Arp2/3-nucleated branched-actin networks [6], possibly by stabilization.

These in vitro results form a strong rationale for studying cortactin in vivo. An in vivo role for cortactin in regulating actin branching is further substantiated by its cellular localization to dynamic-actin assembly sites, such as lamellipodia, endosomes, podosomes and invadopodia [9]. Notably, unlike WASp proteins that localize primarily on membranes, cortactin is more directly localized to cytosolic dynamic actin [4, 9, 10]. Cortactin binds Arp2/3 complex via an N-terminal acidic domain, homologous to that of WASp proteins, and it binds to actin filaments (F-actin) via a tandem-repeats domain [5]. Cortactin also binds to polyproline-stretch-containing proteins, such as WIP, N-WASp, and dynamin, via a C-terminal src homology 3 (SH3) domain [9]. Src phosphorylation sites are located in a C-terminal proline-rich stretch adjacent to the SH3 domain [9].

In this study, we examined the role of cortactin in living cells by using a siRNA/mutant-rescue approach. We find that cortactin promotes cell motility and persistence of lamellipodial protrusion. These functions require simultaneous interaction of cortactin with both the Arp2/3 complex and actin filaments, but not src- or SH3-domain binding partners. Cortactin is recruited to the leading edge of lamellipodia by the Arp2/3 complex and binds preferentially to ATP/ADP-Pi- over ADP-actin filaments. Decreased labeling of uncapped (polymerizable) barbed ends in lamellipodia of cortactin knockdown cells, with unchanged Arp2/3-complex levels, suggests that interactions between cortactin, Arp2/3 complex, and actin filaments lead to enhanced Arp2/3 activity. Finally, cortactin knockdown cells have a selective defect in the rate of formation of new adhesions in lamellipodial protrusions.

Results

Cortactin Knockdown Cells Have Defective Cell Motility and Invasion

A retroviral siRNA expression system, pRetroSuper (pRS) [11], was used to knock cortactin down in HT1080 human fibrosarcoma cells. The siRNA sequence contained a 3 bp mismatch to the mouse gene to facilitate rescue

*Correspondence: alissa.weaver@vanderbilt.edu
[4]Present Address: Department of Biology, Vanderbilt University, Nashville, Tennessee 37232.

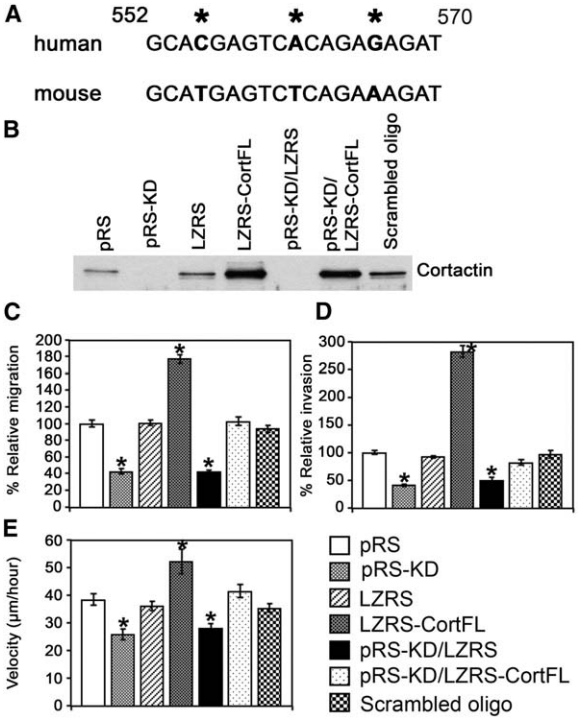

Figure 1. Loss of Cortactin Results in Defective Cellular Migration and Invasion

(A) A 19 bp sequence of human cortactin targeted by siRNA. Mismatches to mouse cortactin are marked by asterisks.

(B) Western blot of cortactin expression levels in control (pRS), knockdown (pRS-KD), overexpression vector only (LZRS), cortactin-overexpressing cells (LZRS-CortFL), knockdown cells rescued with vector only (pRS-KD/LZRS) or with full-length mouse cortactin (pRS-KD/LZRS-CortFL), or cells expressing a scrambled cortactin siRNA oligo (scrambled oligo).

(C) Relative migration through transwell membranes.

(D) Relative invasion though matrigel-coated transwell membranes.

(E) Velocity of cell lines undergoing random motility. Error bars represent standard error of the mean (SEM) from three experiments performed in duplicate (transwell studies) or from n = 50 cells (random motility). * indicates $p < 0.01$, compared to pRS and scrambled oligo control cells.

with mouse constructs (Figure 1A). Cortactin protein expression was reduced by more than 95% in stable polyclonal cell populations (Figure 1B). The LZRS retroviral-expression system [12] was used to overexpress or re-express mouse cortactin in the human cortactin knockdown (pRS-KD) cells (Figure 1B).

Cells lacking cortactin (pRS-KD) show motility defects in three different assays: transwell migration (Figure 1C), transwell invasion (Figure 1D), and random motility (Figure 1E). These defects were rescued by re-expression of mouse wild-type cortactin in the knockdown cells (Figures 1B–1E). In 18 hr transwell-migration assays, 40% of the pRS-KD cells migrated across the filters when compared with control cells. A 2-fold increase in migration was seen in cells overexpressing mouse cortactin (LZRS-CortFL). When the transwell filters were coated with a layer of Matrigel, the results were similar, except that the cortactin-overexpressing cells exhibited an even larger increase (3-fold versus 2-fold) in invasion when compared to control cells (Figure 1D). Cell-motility speed was measured by live-cell imaging of single cells migrating on tissue-culture plastic dishes. Overall cell speed was significantly affected by cortactin knockdown and overexpression (33% decrease and 36% increase compared with control pRS cells, respectively) (Figure 1E, see Supplemental Movies in the Supplemental Data available with this article online). There was no difference in directional persistence of cell migration (Figure S1). The knockdown phenotypes were rescued to 100% that of control cells for the transwell-migration and single-cell velocity assays and to 80% that of controls for transwell invasion by re-expression of full-length mouse cortactin (Figures 1C–1E).

Cortactin Selectively Affects Lamellipodial Persistence

To analyze the role of cortactin in lamellipodial protrusion, we analyzed time-lapse movies of control and pRS-KD cells by kymography. A kymograph represents a timeline of protrusion and allows quantitation of at least four parameters: lamellipodial persistence, protrusion velocity, retraction velocity, and protrusion distance (Figure 2A) [13, 14]. pRS-KD cells exhibited a 2-fold decrease in lamellipodial persistence (the amount of time that a lamellipodia spends protruding before retraction) when compared with vector-only and scrambled-oligo control cells (Figure 2C). There was no difference in other protrusion parameters (Figures 2D–2F). Thus, pRS-KD cells have a selective defect in lamellipodial persistence, a property that previously has been correlated with overall cell speeds [14, 15]. For comparison, movies from WAVE-2 and N-WASp knockdown cells were also analyzed by kymography. Whereas N-WASp knockdown cells had no defect in any lamellipodial protrusion parameters, WAVE-2 knockdown cells were unable to initiate protrusion (Figure S2). These data are consistent with WAVE-2 serving as the initial, essential activator of Arp2/3 complex at the plasma membrane [16–18] and cortactin functioning at either a subsequent stage of lamellipodial protrusion or as an enhancer of WAVE-2 function.

The Arp2/3 and Actin Binding Sites of Cortactin Are Necessary to Rescue Both Motility and Persistence Phenotypes

To determine the minimal binding interactions that could rescue phenotype defects, we re-expressed mouse cortactin fragments and mutant cortactins in the knockdown cells (Figures 3A and 3B). Expression of the N terminus of cortactin (amino acids 1–269) fully rescues the transwell-migration, random-motility, and lamellipodial-protrusion phenotypes of cortactin knockdown cells (Figures 3C, 3D, and 3F). This fragment includes the Arp2/3 and F-actin binding domains but not the src-kinase phosphorylation sites or the SH3 domain (Figure 3A) [5]. Re-expression of full-length mouse cortactin constructs with mutations in either the F-actin (Δ4RP) or Arp2/3-complex binding sites (W22A) [5, 7, 19] did not rescue defects in cellular migration or lamellipodial persistence, despite expression levels that were higher than wild-type cortactin or the N-terminal

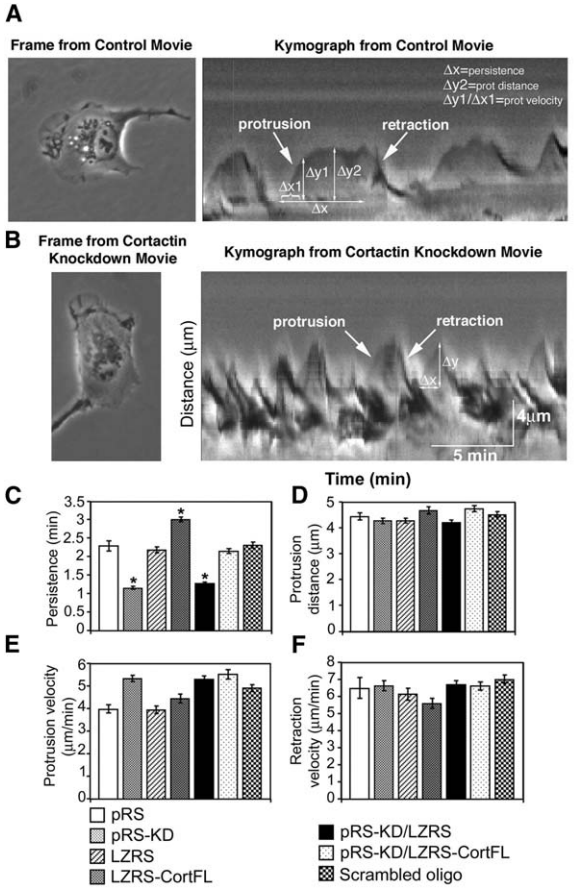

Figure 2. Lamellipodial Persistence Is Decreased in Cortactin Knockdown Cells

Representative kymographs from both control (A) and cortactin knockdown cells (B). Note the definitions in (A) of lamellipodial persistence (Δx), protrusion distance (Δy2), and protrusion velocity (Δy1/Δx1). Scale bars indicate distance and time axes for kymographs. The following are shown: quantification of lamellipodial (C) persistence; (D) protrusion distance; (E) protrusion velocity; and (F) retraction velocity. Error bars represent SEM. * indicates $p < 0.01$, compared to pRS and scrambled oligo control cells, and n = 50 cells.

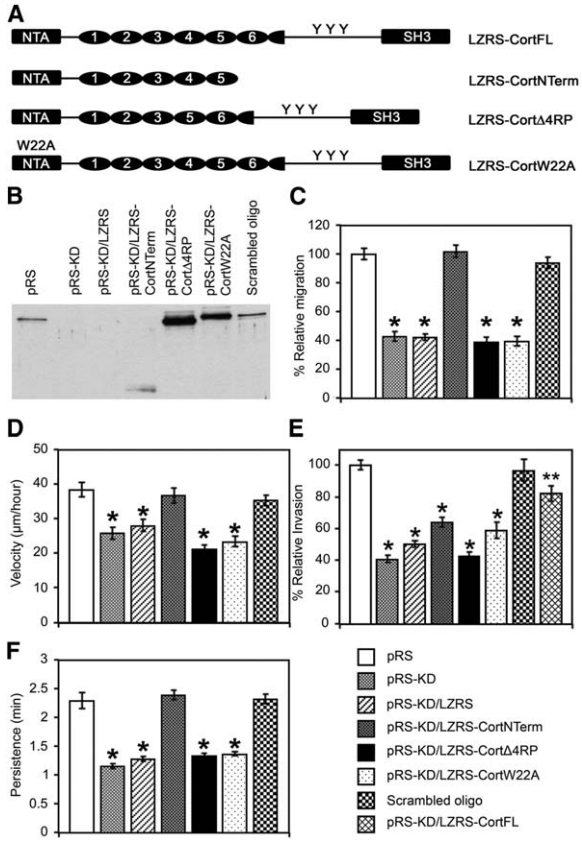

Figure 3. Cell Motility and Lamellipodial Protrusion Depend on Interactions of Cortactin with Both Arp2/3 and F-actin

(A) The following cortactin-rescue constructs are shown: LZRS-Cort-FL (wild-type); LZRS-Cort-NTerm (N-terminus); LZRS-CortΔ4RP (actin binding mutant); LZRS-CortW22A (Arp2/3 binding mutant). The following abbreviations and symbols are used: NTA, N-terminal acidic domain; ovals, cortactin repeat domains; YYY, three src phosphorylation sites; and SH3, src homology 3 domain. These mutations are described in [5, 19].

(B) Western blot showing expression of rescue constructs in cortactin knockdown cells.

(C) Relative migration through transwell membranes. n = 3 with duplicate wells.

(D) Velocity of cell lines undergoing random motility on tissue-culture dishes; $n \geq 50$ cells.

(E) Relative invasion of cortactin cell lines through matrigel-coated transwell membranes. n = 3 with duplicate wells.

(F) Lamellipodial persistence is shown, and $n \geq 50$ cells.

For all experiments (C–F), error bars represent SEM and * indicates $p < 0.01$, when compared to pRS and scrambled oligo cells. For invasion studies (E), * indicates $p < 0.01$, when also compared to pRS-KD/LZRS-Cort-FL, in addition to pRS and scrambled oligo cells. ** indicates $p < 0.05$, when compared to pRS and scrambled oligo cells.

fragment (Figures 3A and 3B). Thus, cortactin must bind both F-actin and Arp2/3 complex to promote persistent lamellipodial protrusion and productive cell motility. In the invasion assay, which requires degradation of extracellular matrix in addition to cell motility, the results were more complex with no rescue by cortactin deficient in F-actin binding and partial rescue by the N-terminal fragment and by cortactin deficient in Arp2/3 binding (Figure 3E).

Cortactin Is Recruited to the Leading Edge Primarily by Interactions with the Arp2/3 Complex

Localization of endogenous cortactin and of mouse cortactin proteins re-expressed in the pRS-KD cells was examined by immunofluorescence (Figure 4). We quantitated enhancement of cortactin proteins at the leading edge in various cell lines by analyzing line scans drawn across the width of lamellipodial protrusions (Figure 4K). The average pixel intensities at a distance 0 and 4 μm from the edge were compared to give a leading-edge ratio (Table S1). Cortactin localization to the leading edge was similar in pRS-KD cells rescued with full-length mouse cortactin (pRS-KD/FL) (Figure 4E) and control cells (pRS) (Figure 4A). In contrast, cortactin that cannot bind Arp2/3 (W22A) does not localize to the leading edge of the cell (Figure 4G, Table S1).

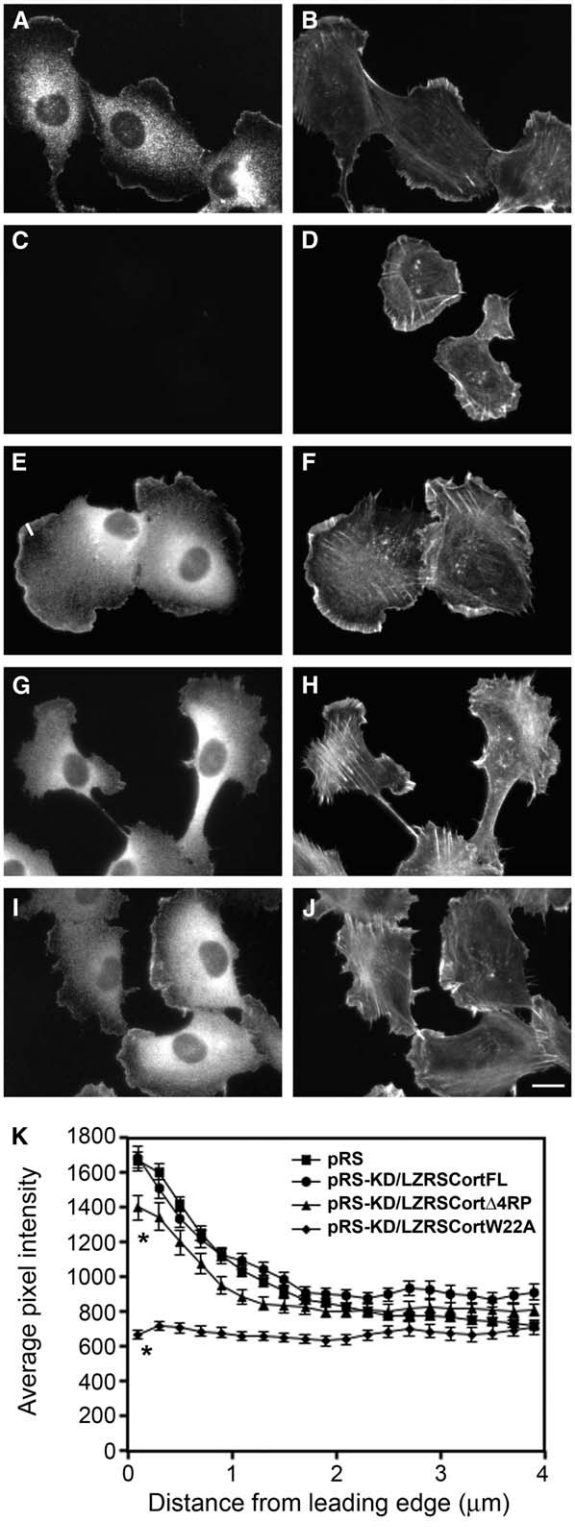

Figure 4. Cortactin Is Recruited to Lamellipodia by Arp2/3 Complex

Cortactin localization in HT1080 cells was assessed by immunofluorescence (A, C, E, G, and I). Alexa-fluor-phalloidin staining shows actin filaments (B, D, F, H, and J). Cell lines are as follows: pRS (A, B), pRS-KD (C, D), pRS-KD/LZRS-CortFL (E, F), pRS-KD/LZRS-W22A (G, H), and pRS-KD/LZRS-Δ4RP (I, J); the scale bar represents 10 μm. (K) Fluorescent-intensity measurements from line scans across the width of lamellipodia (representative line in panel [E]) are shown. Points represent the mean ± SEM from n = 50 cells. * indicates $p < 0.01$ when compared to pRS.

Surprisingly, cortactin that cannot bind actin filaments (Δ4RP) (Figure 4I) localizes to the leading edge, with only a small reduction compared with that of endogenous and re-expressed wild-type cortactin (pRS-KD/FL) (Figure 4K, Table S1). These data indicate that localization of cortactin to HT1080 lamellipodia depends on interactions with Arp2/3 complex. Cortactin binding to F-actin is also important for function because, despite localization to the leading edge (Figure 4), expression of the Δ4RP actin binding mutant was unable to rescue any pRS-KD phenotypes, including invasion (Figure 3).

Cortactin Binds Preferentially to Dynamic-Actin Filaments

Newly polymerized actin filaments are formed from ATP-actin monomers. ATP-F-actin is hydrolyzed to ADP-Pi-F-actin at a rate of 0.3 sec^{-1} [20] followed by release of the inorganic phosphate (Pi) at a rate of 0.002 sec^{-1} to form ADP-F-actin [21]. As a result of this large rate differential, dynamic-actin filaments are composed mainly of both ATP- (from ongoing polymerization) and ADP-Pi-actin (from slow release of the hydrolyzed phosphate), and older actin filaments are composed mainly of ADP-F-actin [1]. The nucleotide state of actin affects the kinetics of actin assembly [1, 22], as well as interactions with certain actin-associated proteins such as cofilin [1, 23]. We tested whether cortactin preferentially binds dynamic actin by performing binding experiments in which purified N-terminal cortactin fragment (100 nM) was incubated with various concentrations of ATP- or ADP-actin filaments. This cortactin fragment is sufficient for proper localization in Rac1-induced lamellipodia [5], can rescue the protrusion and motility phenotypes of pRS-KD cells (Figure 3), and contains the only actin binding site [5]. After the ultracentrifugal sedimentation of actin filaments, bound N-terminal cortactin was calculated from the amount depleted from the supernatants (Figure 5B). The results indicate that N-terminal cortactin has a 15-fold higher affinity for filaments prepared from ATP-actin than for those prepared from ADP-actin (K_d = 0.248 μM versus 3.87 μM, Figure 5A). The K_d for ATP-actin is similar to previous determinations (0.230–0.430 μM) [7, 24]. Because the F-actin prepared from ATP-actin monomer likely contains a mixture of both ATP- and ADP-Pi-F-actin, further experiments were performed with actin polymerized in the presence of beryllium fluoride to mimic ADP-Pi-F-actin and full-length cortactin (70 nM). Cortactin binds to ADP-BeF3-F-actin with a slightly higher affinity than that of ATP-actin (K_d = 0.107 μM versus K_d = 0.273 μM, Figure 5C). These data are consistent with preferential binding of cortactin to dynamic-actin filaments, with the highest apparent affinity for ADP-Pi filaments.

Cortactin Enhances In Vivo Production of Uncapped Barbed Ends of Actin Filaments

Interactions between Arp2/3, cortactin, and dynamic actin may result in stabilization of preexisting branch

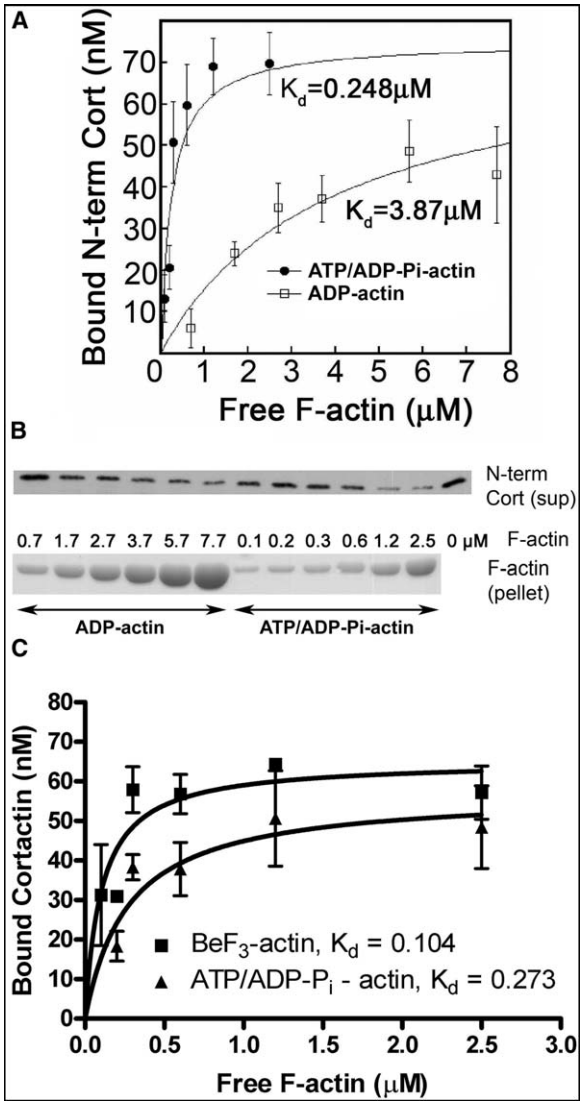

Figure 5. Cortactin Preferentially Binds to Dynamic Actin

(A) Specific equilibrium binding of N-terminal (N-term) cortactin to actin filaments. The data are plotted as the mean ± SEM (n = 7).

(B) Representative Western blot (upper) showing depletion of N-terminal cortactin from supernatants of a cosedimentation experiment. The corresponding Coomassie-stained gel of actin pellets from the cosedimentation experiment is shown below. Concentrations of ADP- and ATP/ADP-Pi-actin filaments for each lane are indicated between the blot and gel.

(C) Specific equilibrium binding of cortactin to actin filaments, as indicated. The data are plotted as the mean ± SEM (n = 3).

points or increased efficiency of branch formation via enhanced Arp2/3 activity [6, 7]. To test an effect on Arp2/3 activity, we examined the incorporation of Alexa-488-actin at the leading edge of saponin-permeabilized cells (Figures 6A–6D). This assay detects the presence of uncapped barbed ends of actin filaments in cells [25, 26]; these barbed ends are a major product of Arp2/3-complex nucleation activity [1]. Cells were serum starved for 30 min, and media+serum was then replenished for 1 min to synchronize protrusion

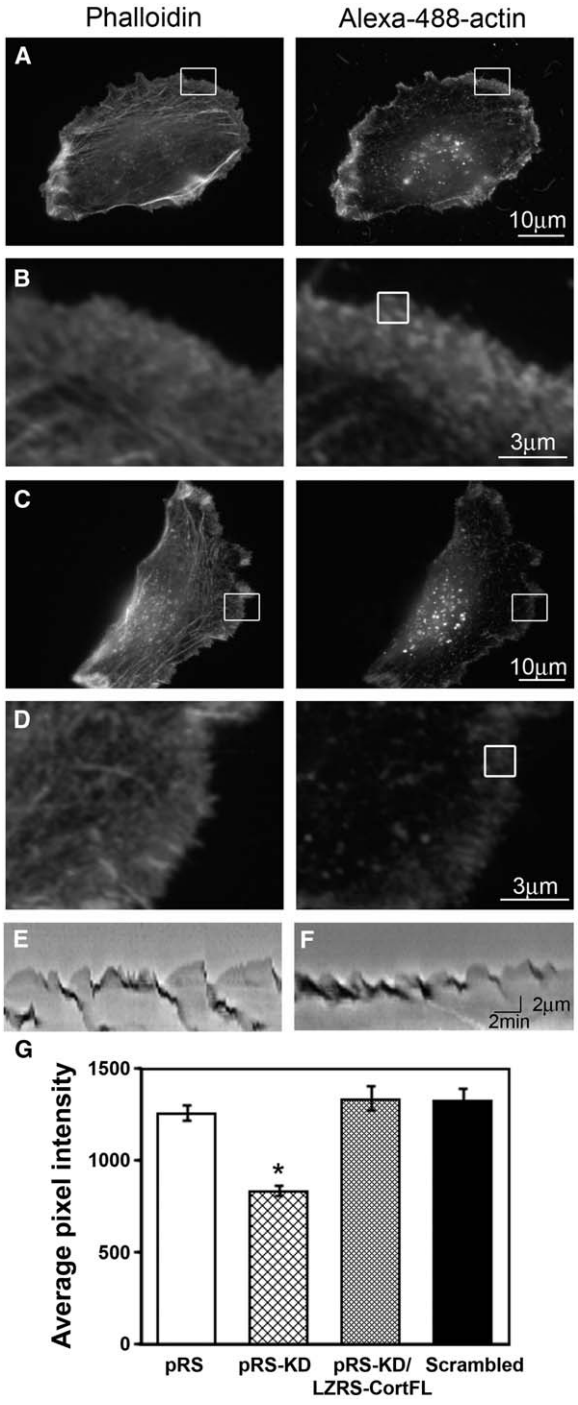

Figure 6. Cortactin Enhances In Vivo Production of Uncapped Barbed Ends of Actin Filaments

(A) shows a representative control cell (pRS). (C) shows a representative pRS-KD cell. White boxes in (A) and (C) indicate regions magnified in (B) and (D). Representative kymographs of pRS (E) and pRS-KD (F) cells treated in the same manner as (A–D) are shown. (G) shows quantification of average pixel intensity of a standardized 2.5 μm^2 square at the leading edge of the lamellipodia in Alexa-488-actin-labeled images from control (pRS and Scrambled), pRS-KD, and pRS/LZRS-CortFL cells (white boxes in [B] and [D] show the size of the square used for quantification). Error bars represent SEM; * indicates $p < 0.01$, n = 65 cells.

before barbed end labeling. Under these conditions, cells have robust protrusion (Figures 6E and 6F). Cells were imaged with identical microscope and camera settings. Quantitation of the average fluorescence intensity at the leading edge indicates that pRS-KD cells have a 34% decrease in Alexa-actin incorporation at the leading edge compared with control and pRS-KD/LZRS-FL-rescued cells (Figure 6G). Thus, cortactin affects the availability of uncapped barbed ends in lamellipodia. There is no difference in Arp2/3-complex localization to lamellipodia, suggesting a change in Arp2/3-complex function (Figure S3). Although not mutually exclusive, these data are more consistent with a role for cortactin in enhancement of Arp2/3-complex activity than in stabilization of preexisting branches.

Cortactin Regulates the Assembly Rate of New Adhesions in Cellular Protrusions

A potential mechanism by which cortactin might enhance lamellipodial persistence and increase cell motility is by promoting the formation of new cellular adhesions in protrusions. This possibility was tested with GFP-paxillin to mark nascent adhesions [27, 28]. Control and pRS-KD cells expressing GFP-paxillin were plated on glass dishes coated with 1 μg/ml fibronectin and allowed to spread for 30 min before movies were taken [27, 28] (Figure 7A, Supplemental Movies). Analysis of fluorescence-intensity changes over time revealed that pRS-KD cells have a selective defect in the assembly rate of new adhesions (Figure 7B, Table 1). There is no significant change in the adhesion disassembly rate (Figure 7C, Table 1). The assembly defect in pRS-KD cells is fully rescued by N-terminal cortactin (Table 1), indicating that interactions with Arp2/3 complex and F-actin are sufficient to promote adhesion assembly. In some experiments, cells were cultured on plastic overnight (the same conditions as the lamellipodial-protrusion assays) and imaged by dual IRM/GFP-paxillin fluorescence. As with cells plated on fibronectin, pRS-KD cells cultured on plastic have a selective defect in adhesion assembly (data not shown). The sites of closest adhesion by IRM colocalized with GFP-paxillin fluorescence (Figure S4).

Discussion

We show that cortactin affects cell motility, most likely through enhancement of lamellipodial persistence. This conclusion is based on analysis of RNAi knockdown cells by live-cell imaging and biochemical approaches. Our main finding is that in reconstitution experiments, both the Arp2/3 and F-actin binding sites are necessary and sufficient to rescue fully the persistence and motility phenotype, suggesting that cortactin forms a molecular bridge between Arp2/3 complex and actin filaments. Mutant-localization data indicate that Arp2/3 complex primarily recruits cortactin to the leading edge of migrating cells. At this site, cortactin preferentially binds newly polymerized actin filaments, as shown by cosedimentation studies assessing its affinity for ATP/ADP-Pi- versus ADP-actin. In situ barbed-end-labeling studies suggest that cortactin boosts Arp2/3-complex activity, either directly or indirectly, in lamellipodia. Together, these data indicate that cortactin regulates Arp2/3-complex-mediated actin assembly in lamellipodia. An intriguing clue as to how cortactin-enhanced actin assembly may lead to lamellipodial persistence and motility is provided by the observation that in knockdown cells, there is a reduction in the rate of new adhesion formation in lamellipodia, as measured by paxillin turnover.

Cortactin Bridges Arp2/3 Complex and Dynamic Actin in Lamellipodia

Two results strongly suggest that cortactin may act as a bridge that tightens Arp2/3-complex association with freshly polymerized actin filaments: First, phenotype rescue in knockdown cells requires recombinant cortactin fragments that simultaneously bind Arp2/3 complex and actin filaments; second, cortactin has higher affinity for ATP/ADP-Pi- than ADP-actin filaments. A bridge mechanism is consistent with previous cosedimentation experiments showing that cortactin strengthens association of Arp2/3 complex with actin filaments [7]. It is not clear, though, whether this cortactin bridge provides a direct activation boost to the Arp complex or adds mechanical strength to actin-network branch points or both. A direct effect on activation is consistent with in vitro data showing that cortactin alone can activate Arp2/3 complex through the same binding domains required for rescuing knockdown cells [6, 7]. It also easily explains the cortactin-dependent increase in free barbed ends we observed in lamellipodia. In this scenario, the cortactin activation boost would likely occur after initial activation of Arp2/3 complex by WAVE proteins because WAVE-2 knockdown cells are unable to initiate lamellipodial protrusion—i.e., their absence preempts cortactin action. In this context, we cannot rule out the possibility that cortactin may augment WAVE-2 activity.

Mechanical strengthening is supported by in vitro data showing preformed branch point stabilization by cortactin [6]. In this respect, it is not known whether cortactin interacts with the mother or daughter filament at an actin branch point. However, because it is recruited early by Arp2/3 complex and may contribute to its activation, it seems more plausible that cortactin strengthens the association of Arp2/3 complex with an ADP-Pi-actin patch on the mother filament. Removal of Pi from aging mother filaments (e.g., by cofilin [20]) could then weaken cortactin-filaments interaction and release the bridge as the network retracts. It is possible to envision other mechanistic scenarios; more experiments are needed to clarify these interactions.

Another point that needs clarification is the spatiotemporal relationship between cortactin and the Arp2/3 complex's main activators, WASp family proteins. Because WASps are strictly located on membranes [4, 10], it is possible that cortactin is recruited by Arp2/3 complex immediately after the newly formed actin branch moves away from the membrane. Alternatively, cortactin might bind Arp2/3 complex simultaneously with WASp proteins at the membrane. Biochemical experiments with N-WASp indicate that under some conditions, cortactin and N-WASp can simultaneously bind Arp2/3 complex [19]. However, it is unknown whether

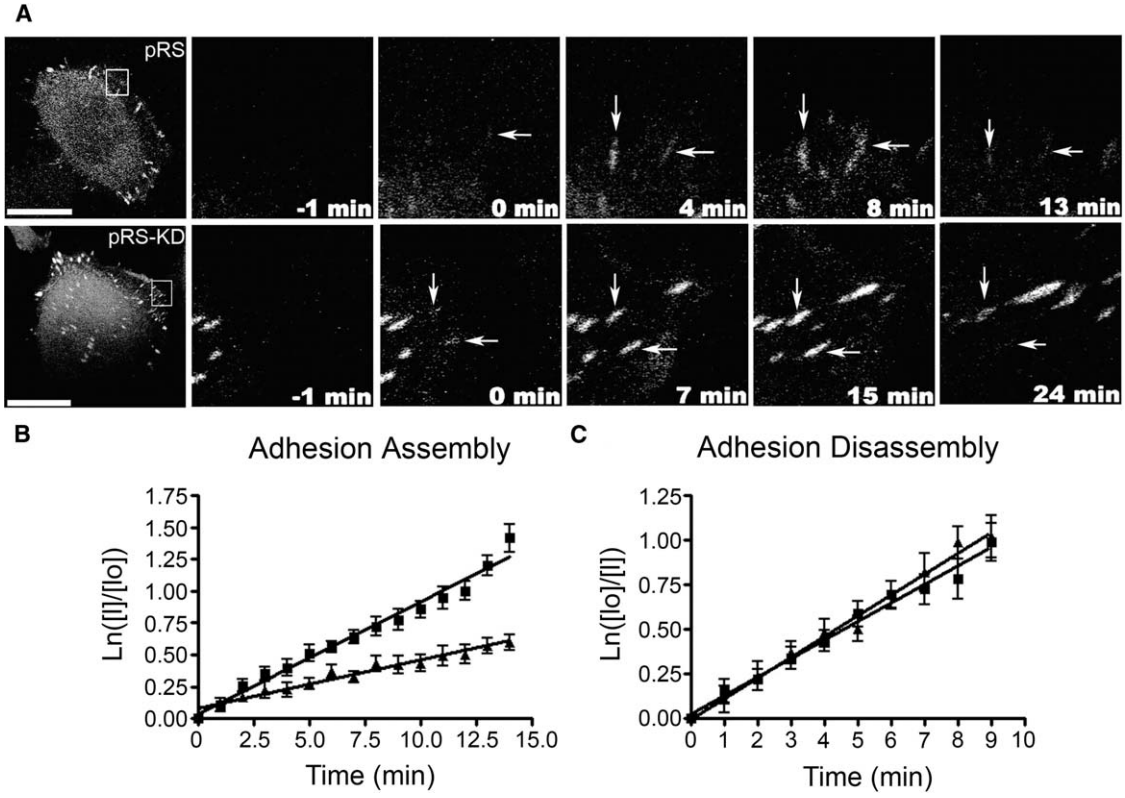

Figure 7. Deficient Adhesion Assembly in Cortactin Knockdown Cells

(A) Time series of GFP-paxillin-marked adhesion assembly and disassembly of pRS (top) and cortactin knockdown (pRS-KD) cells (bottom). Time = 0 indicates start of adhesion. Arrows indicate adhesions. The bar represents 10 μm.

(B and C) Graph of adhesion assembly (B) and disassembly (C) of pRS (closed squares) and pRS-KD cells (closed triangles). Points represent average ± SEM of the natural log of the ratio of the integrated fluorescent intensity at each time point to the initial fluorescent intensity. Measurements were performed on 10 to 15 individual adhesions from 5–7 cells. The slope of the line represents the rate constants of assembly and disassembly of adhesions.

this occurs in vivo or whether WAVE-2, the WASp important for lamellipodial protrusion, functions similarly.

Cortactin Promotes the Formation of New Adhesions in Lamellipodial Protrusions

A decreased rate of adhesion assembly, detected by live-cell imaging of GFP-paxillin turnover, potentially explains both unstable lamellipodial protrusions and reduced random motility. Although the T1/2 for lamellipodial persistence is shorter than the T1/2 for adhesion assembly (2 min versus 8 min), the GFP-paxillin adhesions assembled within 1 μm of cell edges and moved rearward 1–3 μm before disassembly. Thus, sites of new adhesion formation may lead to cell translocation, with new protrusions forming in front of the previous ones. The location of dynamic GFP-paxillin adhesions corresponds well to the lamella (~1–2 μm from the cell edge), a transition zone that is between the lamellipodia and the cell body and where cell-substrate adhesions first couple to actomyosin contractile forces [29]. Stabilization of Arp2/3 complex in actin networks by cortactin may allow direct interaction with and/or recruitment of critical adhesion proteins. Indeed, DeMali et al. reported association of vinculin with Arp2/3 complex un-

Table 1. Assembly and Disassembly Rate Constants and Half-Lives of GFP-Paxillin Adhesions

	Assembly		Disassembly	
	$K_{assembly}$ (min^{-1})	Half-Life (min)	$K_{disassembly}$ (min^{-1})	Half-Life (min)
pRS	0.088 ± 0.003	7.88	0.103 ± 0.004	6.71
pRS-KD	0.038 ± 0.002*	18.2*	0.116 ± 0.002	5.95
pRS-KD/LZRS-CortFL	0.092 ± 0.002	7.56	0.103 ± 0.006	6.71
pRS-KD/LZRS-CortNTerm	0.079 ± 0.014	8.66	0.114 ± 0.004	6.08
Scrambled oligo	0.078 ± 0.007	8.84	0.132 ± 0.011	5.24

Rate constants are reported as the slope ± SEM of average data points from 5–7 cells with 10–15 adhesions per cell. Half-life is reported as Ln2/rate constant. * indicates $p < 0.01$ compared to pRS and scrambled control.

der membrane-protrusion regimes [30]. Alternatively, the rate of adhesion assembly could be secondary to lamellipodial persistence itself—e.g., lamellipodial instability may generally decrease adhesion assembly rates. To our knowledge, this is the first description of a molecular event that affects the assembly rate of GFP-paxillin-labeled adhesions and should prompt studies of how lamellipodial protrusion and Arp2/3 activity affect the assembly of new adhesions.

Function of Other Cortactin Binding Partners

In contrast to lamellipodial protrusion and cell motility, the decreased ability of pRS-KD cells to invade through Matrigel-coated filters is only partially rescued by the N-terminal fragment of cortactin. Thus, there appear to be additional cortactin functions, such as protease secretion or endocytosis, that are used in invasion and require binding interactions at its C terminus. Cortactin binding partners, such as src kinase, N-WASp, or dynamin, that are involved in membrane trafficking and in the formation of invasive structures such as podosomes and invadopodia [31, 32] are obvious candidates for these functions.

A recent study reported that overexpression of cortactin promotes cell motility in scratch assays through N-WASp binding [33]. In our hands, however, the N-WASp binding domain of cortactin was dispensable in single-cell-motility, transwell-migration, and lamellipodial-protrusion rescue assays with pRS-KD cells. Furthermore, inhibition of N-WASp by siRNA or wiskostatin treatment had no effect on any lamellipodial-protrusion parameters. However, it is possible that when cortactin is overexpressed, cortactin and N-WASp function together to regulate other aspects of cell motility, such as cell-cell adhesion or matrix secretion. This may be relevant in the context of tumors that express high levels of cortactin as a result of 11q13 amplification [9].

Additional Cortactin Functions

Finally, cortactin-knockdown phenotypes have been reported in other recent studies and include promoting actin assembly during invasion by Shigella bacteria [34] and strengthening N-cadherin-mediated cell-cell adhesions [35]. Both of those phenotypes, unlike the phenotype reported here, required tyrosine phosphorylation of cortactin. More relevant to our work, two recent studies on actin assembly induced by Salmonella and N-WASp-coated beads, respectively, reported that cortactin knockdown results in increased numbers of lamellipodia [36, 37] and defects in the formation of a single dominant lamellipod [37]. Our finding that cortactin promotes lamellipodial persistence suggests a mechanism for such defects in morphologic polarization. Future studies will address cortactin function in complex cellular processes, such as chemotaxis, that depend on morphologic polarization.

Conclusions

Cortactin promotes cell motility by selectively promoting lamellipodial persistence and adhesion assembly, through interactions with the Arp2/3 complex and actin filaments. Dynamic regulation of actin assembly and lamellipodial protrusion by cortactin may be important in complex motility-dependent processes, such as cancer metastasis, nerve growth cone pathfinding, and immune-cell chemotaxis.

Experimental Procedures

Antibodies and Reagents

4F11 anti-cortactin antibody was previously described [38]. C90 polyclonal antibody was made in chickens, with N-terminal cortactin as the antigen.

Construction of siRNA and Retroviral-Expression Constructs

Sixty-four base pair oligos containing sense and antisense sequences flanking a 6 base hairpin (IDT) were inserted into pRS vector (a kind gift of Reuven Agami, [11]). Parent cortactin vectors have been described previously [5]; the inserts were cloned into LZRS-Neo retroviral-expression vector [12].

Cell-Line Construction and Cell Culture

Human HT1080 cells (ATCC) and Phoenix 293 packaging cells (from Dr. Gary Nolan, Stanford University) were grown in DMEM + 10% BGS (Hyclone). Phoenix 293 cell transfection, viral harvest, and transduction of HT1080 cells were performed as previously described [12]. Cells were selected with 4 μg/ml puromycin (pRS) and/or 600 μg/ml G418 (LZRS-Neo) for 5 days.

Protein Purification

N-terminal cortactin was purified as GST-Nterm cortactin, and this was followed by tag cleavage, removal, and further purification as described [19]. Actin was purified from chicken pectoralis skeletal muscle [39] and gel filtered [22, 40]. ADP-actin was prepared by the hexokinase method [22].

Cortactin-Binding Studies

Cortactin binding to ATP- or ADP-actin filaments was determined with a supernatant depletion assay [19]. ATP-F-actin and ADP-F-actin was prepared from monomers by polymerization in the presence of 80 mM KCl, 2 mM MgCl2, 20 mM HEPES, pH 7.4 (polymerization buffer) for 1 hr at room temperature (RT). BeF3-filaments were polymerized from ATP-actin in the presence of 5 mM NaF and 150 μM BeF3 for 4 hr at RT, as previously described [23]. A 100 nM N-terminal fragment or 70 nM full-length cortactin was incubated with ATP-, BeF3-, or ADP-actin filaments in polymerization buffer. After 10 min at RT, cortactin bound to actin filaments was separated from free cortactin by ultracentrifugation for 20 min at 175,000 × g. Bound cortactin was calculated from the amount depleted from the supernatants; this amount was determined by Western-blot analysis [19]. Binding results were plotted as bound Cortactin versus free F-actin and were fit by the following equation:

$$[\text{F-actin}_{\text{bound}}] = \{(K_d + [\text{Cortactin}] + [\text{F-actin}]) - \sqrt{(K_d + [\text{Cortactin}] + [\text{F-actin}])^2 - (4[\text{Cortactin}][\text{F-actin}])}\}/2$$

$[\text{F-actin}_{\text{bound}}]$ was assumed to equal $[\text{Cortactin}_{\text{bound}}]$. Statistical analysis was performed with Kaleidograph software.

Transwell-Migration and Invasion Assays

Cell-migration and Matrigel-invasion assays were performed with 8.0 μm pore transwell or Biocoat Matrigel-invasion chambers (BD Transduction Laboratories) according to the manufacturer's protocol. Assays were performed over 18 hr with 10% BGS + 5% Nuserum DMEM as an attractant. The number of cells that had migrated/invaded was determined by counting five random areas over a grid pattern from duplicate chambers in three separate experiments.

Immunofluorescence

We plated 3 × 10^4 cells/cm^2 onto glass coverslips coated with 50 μg/ml fibronectin. After 24 hr, the cells were fixed with 3.7% paraformaldehyde, permeabilized with 0.4% Triton-X-100, and blocked with 3% BSA. A 3 nM AlexaFluor-594 Phalloidin (Molecular Probes) was used for F-actin detection. 4F11 antibody (1:500) was used for

cortactin staining. Immunofluorescence was visualized on a Zeiss Axioplan 2 microscope with 63× Plan-Apochromat, 1.4 NA or 40× F Fluar, 1.3 NA oil immersion objectives. Images were captured on a Hamamatsu Orca-ER camera with OpenLab software. Line scans were performed in Metamorph with a 1-pixel-wide line, and fluorescence intensity was measured every 0.2 μm.

Live-Cell Imaging

Live-cell imaging was performed on a Zeiss Axiovert 200M microscope at 37°C with 5% CO_2, with a Hamamatsu Orca-ER camera and OpenLab software. For phase-contrast microscopy, 3×10^4 cells/cm^2 were plated into 6-well plates and incubated overnight. Prior to imaging, the medium was replaced with fresh DMEM + 10% BGS. For single-cell velocity studies, images were taken with a 10×/0.30 plan neofluar ph1 objective lens every 5 min for a total of 4.5 hr. Images for kymography analysis were taken with a 40× LD-Achroplan Korr ph2, 0.6 NA objective lens every 6 s for a total of 20 min. Kymographs were analyzed with Metamorph and Excel software.

For fluorescence microscopy, cells were transfected with paxillin-GFP and sorted by FACS to obtain cells with low GFP-fusion-protein expression. Cells were plated onto glass-bottom dishes coated with 1 μg/ml fibronectin and allowed to adhere for 30 min prior to imaging. Images were acquired with either a Perkin Elmer Spinning Disk Confocal microscope or a Zeiss LSM510 confocal microscope with a 100× PlanApo, 1.3 NA objective at 37°C. Cells were imaged every 30 s for 30–45 min.

Adhesion assembly and disassembly analysis was performed as previously described [27, 28]. Metamorph was used to measure the integrated fluorescent intensity from individual adhesions in cells expressing GFP-paxillin (corrected for background). The rate constants for assembly and disassembly of adhesions were determined from the slope of the plot of the natural log of fluorescent intensity over time. The half-life of adhesion assembly or disassembly was determined as Ln2/rate constant.

Barbed-End Labeling

Cells were serum starved for 30 min and then stimulated with 10% BGS, 5% Nu-Serum for 1 min. The cells were permeabilized with saponin buffer (20 mM HEPES, 138 mM KCl, 4 mM $MgCl_2$, 3 mM EGTA, 0.2mg/ml saponin, 1% BSA, 1 mM ATP, 3 μM phalloidin) for 1 min, washed once in saponin-free buffer, and labeled for 3 min at 37°C with 0.4 μM Alexa-488-actin (Molecular Probes). The cells were fixed and counterstained with Alexa-594-phalloidin. Quantification of the level of barbed-end labeling in the lamellipodia was performed by measuring the pixel intensity in a standardized 2.5 μm^2 (1.25 μm × 1.25 μm) square at the edge of the lamellipodia in Alexa-488-actin-labeled images, with Metamorph software.

Supplemental Data

Supplemental Data include Supplemental Experimental Procedures, four Supplemental Figures, one Supplemental Table, and eight Supplemental Movies and are available with this article online at http://www.current-biology.com/cgi/content/full/15/14/1276/DC1/.

Acknowledgments

This work was supported by NIH K22 CA109590-01 and Vanderbilt Development Funds to A.M.W. Donna Webb was supported by GM23244 (to Rick Horwitz). Experiments were performed in part through the use of the VUMC Cell Imaging Shared Resource and the VUMC Flow Cytometry core. The authors wish to thank Dr. Vito Quaranta for critical reading of the manuscript; Drs. Chang Chung and Irina Kaverina for helpful suggestions; and Nichole Lobdell, Dr. Jerome Jourquin, and Gregg Wildenberg for technical advice.

Received: March 17, 2005
Revised: June 14, 2005
Accepted: June 15, 2005
Published: July 26, 2005

References

1. Pollard, T.D., and Borisy, G.G. (2003). Cellular motility driven by assembly and disassembly of actin filaments. Cell *112*, 453–465.
2. Mullins, R.D., Heuser, J.A., and Pollard, T.D. (1998). The interaction of Arp2/3 complex with actin: Nucleation, high affinity pointed end capping, and formation of branching networks of filaments. Proc. Natl. Acad. Sci. USA *95*, 6181–6186.
3. Higgs, H.N., Blanchoin, L., and Pollard, T.D. (1999). Influence of the C terminus of Wiskott-Aldrich syndrome protein (WASp) and the Arp2/3 complex on actin polymerization. Biochemistry *38*, 15212–15222.
4. Millard, T.H., Sharp, S.J., and Machesky, L.M. (2004). Signalling to actin assembly via the WASP (Wiskott-Aldrich syndrome protein)-family proteins and the Arp2/3 complex. Biochem. J. *380*, 1–17.
5. Weed, S.A., Karginov, A.V., Schafer, D.A., Weaver, A.M., Kinley, A.W., Cooper, J.A., and Parsons, J.T. (2000). Cortactin localization to sites of actin assembly in lamellipodia requires interactions with F-actin and the Arp2/3 complex. J. Cell Biol. *151*, 29–40.
6. Weaver, A.M., Karginov, A.V., Kinley, A.W., Weed, S.A., Li, Y., Parsons, J.T., and Cooper, J.A. (2001). Cortactin promotes and stabilizes Arp2/3-induced actin filament network formation. Curr. Biol. *11*, 370–374.
7. Uruno, T., Liu, J., Zhang, P., Fan Yx, Y., Egile, C., Li, R., Mueller, S.C., and Zhan, X. (2001). Activation of Arp2/3 complex-mediated actin polymerization by cortactin. Nat. Cell Biol. *3*, 259–266.
8. Kinley, A.W., Weed, S.A., Weaver, A.M., Karginov, A.V., Bissonette, E., Cooper, J.A., and Parsons, J.T. (2003). Cortactin Interacts with WIP in Regulating Arp2/3 Activation and Membrane Protrusion. Curr. Biol. *13*, 384–393.
9. Daly, R.J. (2004). Cortactin signalling and dynamic actin networks. Biochem. J. *382*, 13–25.
10. Zettl, M., and Way, M. (2001). New tricks for an old dog? Nat. Cell Biol. *3*, E74–E75.
11. Brummelkamp, T.R., Bernards, R., and Agami, R. (2002). Stable suppression of tumorigenicity by virus-mediated RNA interference. Cancer Cell *2*, 243–247.
12. Ireton, R.C., Davis, M.A., van Hengel, J., Mariner, D.J., Barnes, K., Thoreson, M.A., Anastasiadis, P.Z., Matrisian, L., Bundy, L.M., Sealy, L., et al. (2002). A novel role for p120 catenin in E-cadherin function. J. Cell Biol. *159*, 465–476.
13. Hinz, B., Alt, W., Johnen, C., Herzog, V., and Kaiser, H. (1999). Quantifying lamella dynamics of cultured cells by SACED, a new computer-assisted motion analysis. Exp. Cell Res. *251*, 234–243.
14. Bear, J., Svitkina, T., Krause, M., Schafer, D., Loureiro, J., Strasser, G., Maly, I., Chaga, O., Cooper, J., Borisy, G., et al. (2002). Antagonism between Ena/VASP proteins and actin filament capping regulates fibroblast motility. Cell *109*, 509–521.
15. Bear, J.E., Loureiro, J.J., Libova, I., Fassler, R., Wehland, J., and Gertler, F.B. (2000). Negative regulation of fibroblast motility by Ena/VASP proteins. Cell *101*, 717–728.
16. Yan, C., Martinez-Quiles, N., Eden, S., Shibata, T., Takeshima, F., Shinkura, R., Fujiwara, Y., Bronson, R., Snapper, S.B., Kirschner, M.W., et al. (2003). WAVE2 deficiency reveals distinct roles in embryogenesis and Rac-mediated actin-based motility. EMBO J. *22*, 3602–3612.
17. Yamazaki, D., Suetsugu, S., Miki, H., Kataoka, Y., Nishikawa, S., Fujiwara, T., Yoshida, N., and Takenawa, T. (2003). WAVE2 is required for directed cell migration and cardiovascular development. Nature *424*, 452–456.
18. Innocenti, M., Zucconi, A., Disanza, A., Frittoli, E., Areces, L.B., Steffen, A., Stradal, T.E., Di Fiore, P.P., Carlier, M.F., and Scita, G. (2004). Abi1 is essential for the formation and activation of a WAVE2 signalling complex. Nat. Cell Biol. *6*, 319–327.
19. Weaver, A.M., Heuser, J.E., Karginov, A.V., Lee, W.L., Parsons, J.T., and Cooper, J.A. (2002). Interaction of cortactin and N-WASp with Arp2/3 complex. Curr. Biol. *12*, 1270–1278.
20. Blanchoin, L., and Pollard, T.D. (2002). Hydrolysis of ATP by polymerized actin depends on the bound divalent cation but not profilin. Biochemistry *41*, 597–602.
21. Pollard, T.D., Blanchoin, L., and Mullins, R.D. (2000). Molecular mechanisms controlling actin filament dynamics in nonmuscle cells. Annu. Rev. Biophys. Biomol. Struct. *29*, 545–576.
22. Pollard, T.D. (1986). Rate constants for the reactions of ATP- and ADP-actin with the ends of actin filaments. J. Cell Biol. *103*, 2747–2754.

23. Blanchoin, L., Pollard, T.D., and Mullins, R.D. (2000). Interactions of ADF/cofilin, Arp2/3 complex, capping protein and profilin in remodeling of branched actin filament networks. Curr. Biol. *10*, 1273–1282.
24. Wu, H., and Parsons, J.T. (1993). Cortactin, an 80/85-kilodalton pp60src substrate, is a filamentous actin-binding protein enriched in the cell cortex. J. Cell Biol. *120*, 1417–1426.
25. Symons, M.H., and Mitchison, T.J. (1991). Control of actin polymerization in live and permeabilized fibroblasts. J. Cell Biol. *114*, 503–513.
26. Chan, A.Y., Raft, S., Bailly, M., Wyckoff, J.B., Segall, J.E., and Condeelis, J.S. (1998). EGF stimulates an increase in actin nucleation and filament number at the leading edge of the lamellipod in mammary adenocarcinoma cells. J. Cell Sci. *111*, 199–211.
27. Laukaitis, C.M., Webb, D.J., Donais, K., and Horwitz, A.F. (2001). Differential dynamics of alpha 5 integrin, paxillin, and alpha-actinin during formation and disassembly of adhesions in migrating cells. J. Cell Biol. *153*, 1427–1440.
28. Webb, D.J., Donais, K., Whitmore, L.A., Thomas, S.M., Turner, C.E., Parsons, J.T., and Horwitz, A.F. (2004). FAK-Src signalling through paxillin, ERK and MLCK regulates adhesion disassembly. Nat. Cell Biol. *6*, 154–161.
29. Ponti, A., Machacek, M., Gupton, S.L., Waterman-Storer, C.M., and Danuser, G. (2004). Two distinct actin networks drive the protrusion of migrating cells. Science *305*, 1782–1786.
30. DeMali, K.A., Barlow, C.A., and Burridge, K. (2002). Recruitment of the Arp2/3 complex to vinculin: Coupling membrane protrusion to matrix adhesion. J. Cell Biol. *159*, 881–891.
31. Schafer, D.A. (2002). Coupling actin dynamics and membrane dynamics during endocytosis. Curr. Opin. Cell Biol. *14*, 76–81.
32. Linder, S., and Aepfelbacher, M. (2003). Podosomes: Adhesion hot-spots of invasive cells. Trends Cell Biol. *13*, 376–385.
33. Kowalski, J.R., Egile, C., Gil, S., Snapper, S.B., Li, R., and Thomas, S.M. (2005). Cortactin regulates cell migration through activation of N-WASP. J. Cell Sci. *118*, 79–87.
34. Bougneres, L., Girardin, S.E., Weed, S.A., Karginov, A.V., Olivo-Marin, J.C., Parsons, J.T., Sansonetti, P.J., and Van Nhieu, G.T. (2004). Cortactin and Crk cooperate to trigger actin polymerization during Shigella invasion of epithelial cells. J. Cell Biol. *166*, 225–235.
35. El Sayegh, T.Y., Arora, P.D., Laschinger, C.A., Lee, W., Morrison, C., Overall, C.M., Kapus, A., and McCulloch, C.A. (2004). Cortactin associates with N-cadherin adhesions and mediates intercellular adhesion strengthening in fibroblasts. J. Cell Sci. *117*, 5117–5131.
36. Unsworth, K.E., Way, M., McNiven, M., Machesky, L., and Holden, D.W. (2004). Analysis of the mechanisms of Salmonella-induced actin assembly during invasion of host cells and intracellular replication. Cell. Microbiol. *6*, 1041–1055.
37. Kempiak, S.J., Yamaguchi, H., Sarmiento, C., Sidani, M., Ghosh, M., Eddy, R.J., Desmarais, V., Way, M., Condeelis, J.S., and Segall, J.E. (2005). A neural Wiskott-Aldrich Syndrome protein-mediated pathway for localized activation of actin polymerization that is regulated by cortactin. J. Biol. Chem. *280*, 5836–5842.
38. Wu, H., Reynolds, A.B., Kanner, S.B., Vines, R.R., and Parsons, J.T. (1991). Identification and characterization of a novel cytoskeleton-associated pp60src substrate. Mol. Cell. Biol. *11*, 5113–5124.
39. Spudich, J.A., and Watt, S. (1971). The regulation of rabbit skeletal muscle contraction. I. Biochemical studies of the interaction of the tropomyosin-troponin complex with actin and the proteolytic fragments of myosin. J. Biol. Chem. *246*, 4866–4871.
40. MacLean-Fletcher, S., and Pollard, T.D. (1980). Identification of a factor in conventional muscle actin preparations which inhibits actin filament self-association. Biochem. Biophys. Res. Commun. *96*, 18–27.